A novel computationally efficient Galileo E1 OS acquisition method for GNSS software receiver

Myriam Foucras, Olivier Julien, Christophe Macabiau, Bertrand Ekambi

A Novel Computationally Efficient Galileo E1 OS Acquisition Method for GNSS Software Receiver

Myriam FOUCRAS, *ABBIA GNSS Technologies / ENAC, France*
Olivier JULIEN, *ENAC, France*
Christophe MACABIAU, *ENAC, France*
Bertrand EKAMBI, *ABBIA GNSS Technologies, France*

BIOGRAPHIES

Myriam FOUCRAS received her Masters in Mathematical engineering and Fundamental Mathematics from University of Toulouse in 2009 and 2010. Since 2011, she is a PhD. student at the Signal Processing and Navigation research group of the TELECOM laboratory of ENAC (Ecole Nationale de l'Aviation Civile). Her work is funded by ABBIA GNSS Technologies, in Toulouse, France working on the development of a GPS/Galileo software receiver.

Olivier JULIEN is the head of the Signal Processing and Navigation research group of the TELECOM laboratory of ENAC, in Toulouse, France. His research interests are GNSS receiver design, GNSS multipath and interference mitigation and GNSS interoperability. He received his engineer degree in 2001 in digital communications from ENAC and his PhD in 2005 from the Department of Geomatics Engineering of the University of Calgary, Canada.

Christophe MACABIAU graduated as an electronics engineer in 1992 from the ENAC in Toulouse, France. Since 1994, he has been working on the application of satellite navigation techniques to civil aviation. He received his PhD. in 1997 and has been in charge of the TELECOM laboratory of the ENAC since 2011.

Bertrand EKAMBI graduated by a Master in Mathematical Engineering in 1999. Since 2000, he is involved in the main European GNSS projects: EGNOS and GALILEO. He is the founder manager of ABBIA GNSS Technologies, a French SME working on Space Industry, based in Toulouse, France.

ABSTRACT

The deployment of the European global navigation satellite system, Galileo, with its specific signal structure, encourages the development of new signal processing methods at the receiver level. In particular, the structure and characteristics of the Galileo E1 OS signal make its acquisition not easy and require optimization to reduce computation time and complexity.

The present article proposes a novel Galileo E1 OS signal acquisition method. The background technique to do so is taken from an existing GPS L1 signal acquisition method, the Double Block Zero Padding (DBZP). This paper provides the detailed description (including the mathematical model) of the DBZP and shows its theoretical performance in terms of probability of detection and number of operations. Based on this analysis, the paper proposes an improvement of the DBZP for signals, like Galileo E1 OS, that include frequent bit transitions. This technique is compared with a reference acquisition method, and shows very good and interesting results demonstrating the potential of this innovative Galileo E1 OS signal acquisition method.

INTRODUCTION

The overall context of this work is the development of a GPS/Galileo single frequency (L1) software receiver. This GNSS receiver is meant for educational and research purposes, then the software technology is well adapted due to its reconfigurable nature and important flexibility. The software can be upgraded (tracking of news signals, algorithm changes, and manipulations by students…) without having to modify the hardware. The reduction in material cost without loss of performance is therefore considerable.

The efficient and fast acquisition of Galileo E1 OS signal is still a challenge compared to the acquisition of GPS L1 C/A due to:

- The use of a data and a pilot component (thus splitting the overall signal power towards these two components)
- The fact that the duration of the data and pilot spreading codes is equal to that of a navigation data bit (on the data component), and of that of a secondary code bit on the pilot component
- The duration and length of the spreading codes that is 4 times that of GPS L1 C/A spreading codes

As a consequence, the typical acquisition technique used in mass market GPS/ Galileo L1 receivers signals tends to first acquire the GPS L1 C/A signals, and then, with the information provided by the acquisition of GPS L1

signals, to acquire the Galileo E1 OS signal. Because relying on GPS L1 C/A as a first step to acquire efficiently Galileo E1 OS signals does not appear satisfactory, this article investigates a technique to efficiency and independently acquire Galileo E1 OS signal. The objective is to optimize the software processing to reduce the consumption needs and the computation time. Moreover, two GPS/Galileo receiver features are set, such as on one hand the cold start (first position) is had in less than 1 minute and on the other hand the acquisition of Galileo signals with a received C/N_0 of 27 dBHz should be done 90% of time. These values were fixed after a review of the specifications of currently sold receivers (Receiver surveys sponsored by Novatel in [GPS World, 2011] and [GPS World, 2012]).

An acquisition technique which seems adapted to these purposed due to its efficiency and computational speed is the Double Block Zero Padding (DBZP). The DBZP was shown to have interesting computational performance for the acquisition of GPS L1 C/A signal, although its actual acquisition performance was not reported in the literature. Moreover, the algorithm needs to be adapted to the Galileo E1 OS signal because the structure and features of the Galileo E1 OS signal differ from these of GPS L1 C/A.

The outline of the paper is as follows:

- In the first part, GPS L1 C/A and Galileo E1 OS signals features are reviewed as well as different acquisition methods adapted to these signals.
- The second part describes the Double Block Zero Padding (DBZP) technique, by presenting its strength and limitations. Although, this acquisition method is known, to the best of our knowledge, the mathematical model of the DBZP and its performance have never been derived before and represents one of the innovative contribution of this paper.
- The third section focuses on our new Galileo E1 OS acquisition method, the Double Block Zero Padding Transition Insensitive (DBZPTI).
- A performance study of the DBZPTI is discussed in the fourth part by comparing the performance of our method to a reference acquisition method.

I. STATE-OF-THE-ART OF GPS L1 C/A AND GALILEO E1 OS ACQUISITION TECHNIQUES

This paper deals with an adaptation of a GPS L1 C/A signal acquisition method to the Galileo E1 OS signal. The motivation behind this investigation is to show that even though the structure and characteristics of the GPS L1 C/A and Galileo E1 OS signals are different, the same kind of acquisition methods can be used for the acquisition of the two signals. So it is important to understand what elements have to be considered in order to define this new Galileo E1 OS acquisition method. This section summarizes the GPS L1 C/A and Galileo E1 OS signal characteristics and GPS and Galileo acquisition methods.

Galileo and GPS signals characteristics

The two signals of interest are GPS L1 C/A and Galileo E1 OS. These two signals are in the L1 band and their center frequency is 1575.42 MHz. The technical characteristics of the Galileo E1 OS signal as well as the GPS L1 C/A signal ones are given in the Table 1. The main features of the Galileo E1 OS signal (different from the GPS L1 C/A signal) are:

- The presence of two components in the Galileo E1 OS signal (a data component containing the navigation message and the dataless pilot component) whereas there is only a data component in the GPS L1 C/A signal. The Galileo E1 OS pilot component is characterized by a known secondary code that modulates the primary spreading code. The two components are synchronized.
- The Galileo E1 OS spreading codes' periods have the same duration as a data or secondary code bit. This implies that a transition (data bit and/or secondary code bit) occurs at each spreading code period with a probability of 50%.
- The modulation of the Galileo E1 OS signal is CBOC(6,1,1/11).
- The Galileo E1 OS data bit rate is 250 bps meaning a data bit duration of 4 ms.

Table 1 - GPS L1 C/A and Galileo E1 OS signal technical characteristics

GNSS system	GPS	Galileo	
Service name	C/A	E1 OS	
Spreading modulation	BPSK	CBOC(6,1,1/11)	
Carrier frequency	1.023 MHz	1.023 MHz and 6.138 MHz (2 sub-carriers)	
Code frequency	1.023 MHz	1.023 MHz	
Signal component	Data	Data	Pilot
Code family	Gold codes	Memory codes	
Primary code length	1023	4092	
Secondary code length	-	-	25
Symbol rate	-	-	250 bps
Data rate	50 bps	250	-
Minimum received power	-158.5 dBW	-157 dBW	

As we can see in the Table 1, the data rates for the two signals are different and this point is crucial for the acquisition. Indeed, a data bit transition can occur every 4 ms for a Galileo E1 OS signal compared to 20 ms for a GPS L1 C/A signal. This means that the integration time must be shorter for Galileo signal acquisition or that the acquisition method should thus be robust to data transition bit.
The Galileo spreading code period is four times longer than this GPS spreading code period which means that the acquisition search space is larger (more code delay and Doppler frequency bins) for Galileo acquisition. Due to the presence of sub-carriers in the Galileo E1 OS signal, the autocorrelation functions of the GPS L1 C/A and Galileo E1 OS differ quite significantly. Indeed, the two Galileo signal sub-carriers $p_{CBOC,D}$ for the data component and $p_{CBOC,P}$ for the pilot component can be expressed as:

$$p_{CBOC,D}(k) = \frac{\sqrt{10}\, sign(\sin(2\pi f k T_s)) + sign(\sin(2\pi 6 f k T_s))}{\sqrt{11}}$$
$$p_{CBOC,P}(k) = \frac{\sqrt{10}\, sign(\sin(2\pi f k T_s)) - sign(\sin(2\pi 6 f k T_s))}{\sqrt{11}}$$

Equation 1

where

- $p_{CBOC,D}$ and $p_{CBOC,P}$ are the sub-carriers carried by the data and pilot components
- k is the sample
- $f = 1.023\ MHz$ is the sub-carrier frequency
- T_s is the sampling period

The expressions of the GPS L1 C/A and Galileo E1 OS signals (for one satellite) are given hereafter.
For the GPS L1 C/A signal, it is:

$$r(k) = Ad(k)c(k)cos(2\pi(f_{IF} + f_D)k + \phi) + n(k)$$

Equation 2

where

- r is the received signal
- $A = \sqrt{2P}$ is the amplitude of the signal
- d is the data sequence
- c is the spreading sequence (PRN code)
- f_{IF} is the intermediate frequency
- f_D is the Doppler frequency of the incoming signal
- ϕ is the phase
- n is the noise (including interferences and assumed white Gaussian)

For the Galileo E1 OS signal, it is:

$$r(k) = A\left[d(k)c_{1,D}(k)p_{CBOC,D}(k) - c_2(k)c_{1,P}(k)p_{CBOC,P}(k)\right] \times cos(2\pi(f_{IF} + f_D)k + \phi) + n(k)$$

Equation 3

where

- c_2 is the known secondary code
- $A = \sqrt{P}$ is the amplitude of the signal on each component

The first part in the expression of incoming Galileo E1 OS signal $d(k)c_{1,D}(k)p_{CBOC,D}(k)$ represents the data component with the navigation message and the spreading code including the subcarrier. The second term $c_2(k)c_{1,P}(k)p_{CBOC,P}(k)$ represents the pilot component with the secondary code and a different spreading code. The carrier is expressed by $cos(2\pi(f_{IF} + f_D)k + \phi)$ which depends on the incoming Doppler frequency.

GPS L1 C/A acquisition methods

The goal of the acquisition process is to detect the presence of the useful signal and give a rough estimate of its main parameters (code delay and Doppler frequency) in order to start the tracking process. For this, a correlation process is used to allow the detection of a GNSS signal by the detection of its power. Each signal is processed separately, as each signal requires a correlation with its own spreading code locally generated.
The theory of this traditional acquisition method is widely developed and can be found in [Spilker et al., 1996] or [Borre et al., 2007] and a general scheme is given by the Figure 1.

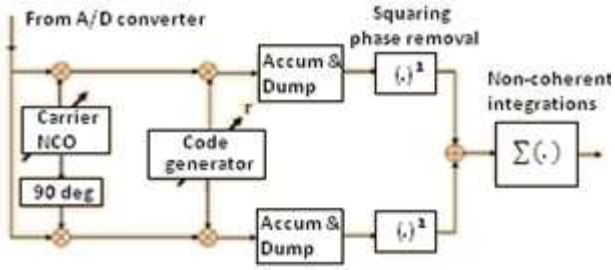

Figure 1– Scheme of the classical acquisition

If there is no information on the signal code delay and Doppler frequency, the traditional acquisition technique consists in constructing an acquiring grid with all possible code delay and Doppler frequency and visiting all the code delay and Doppler frequency bins. The size of this grid is defined by the level of uncertainty on the code delay and the Doppler frequency, as well as the offset between two consecutive values of the possible code delays and Doppler frequencies. For each grid cell (corresponding to one code delay and one Doppler frequency), a local replica is built and correlated with the incoming signal. After that, the integration and dump process gives the correlator output. The expression of the correlator outputs is (given among other in [Julien, 2008] and [Chibout, 2008]):

$$I(k) = \frac{A(k)}{2} d(k) R\left(\varepsilon_\tau(k)\right) sinc\left(\pi \varepsilon_{f_D}(k) T_I\right) cos\left(\varepsilon_\phi(k)\right) + n_I(k)$$
$$Q(k) = \frac{A(k)}{2} d(k) R\left(\varepsilon_\tau(k)\right) sinc\left(\pi \varepsilon_{f_D}(k) T_I\right) sin\left(\varepsilon_\phi(k)\right) + n_Q(k)$$

Equation 4

where

- I is the in-phase correlator output
- Q is the quadrature correlator output
- R is the autocorrelation function
- T_I is the integration time
- $\varepsilon_\tau = |\tau - \hat{\tau}|$ is the error on the code delay
- $\varepsilon_{f_D} = \left|f_D - \widehat{f_D}\right|$ is the error on the Doppler frequency
- $\varepsilon_\phi = \left|\phi - \hat{\phi}\right|$ is the error on the phase
- n_I and n_Q are the in-phase and quadrature correlator output noises

The acquisition criterion is then generally taken as:

$$T = I^2(k) + Q^2(k)$$
$$= \frac{A^2}{4} R^2\left(\varepsilon_\tau(k)\right) sinc^2\left(\pi \varepsilon_{f_D}(k) T_I\right) + n_I^2(k) + n_Q^2(k)$$

Equation 5

As can be seen in Eq. 4 and Eq. 5, the acquisition criterion has a significant value only if the code delay and Doppler frequency of the local replica match those of the received signal. If the criterion goes above a predefined threshold, it means that either the code delay and Doppler frequency are well estimated or it is a false alarm (due to noise for example). The details on how to compute the threshold are developed later on.

From this traditional technique and to reduce the computation time, the circular correlation was developed [Van Nee & Coenen, 1991]. It allows evaluating the correlator outputs faster than the classical (linear search) method. It consists in taking the inverse Fourier transform of the Fourier transform of the incoming signal multiplied by the complex conjugate of the Fourier transform of the spreading code locally generated. It allows saving a considerable amount of time due to the use of optimized FFT algorithms, for example the radix-2 Cooley Tukey algorithm. The development of the mathematical model is detailed in Appendix C. It rests on the fact that the expression of the entire correlation function (for all the code delays) can be expressed as decomposition in Fourier series:

$$R(m) = \frac{1}{N} \sum_{l=0}^{N-1} c(l) c(l-m)$$
$$= \frac{1}{N} IFFT\left(FFT\left(c(k)\right) \overline{FFT}(c(k))\right)$$

Equation 6

If this result is applied for the correlator output computation (the noise is not taken), it leads to (after computation presented in Appendix D):

$$IFFT\left(FFT\left(r(t)\right) \overline{FFT}\left(c(t)\right)\right)(j)$$
$$= \frac{1}{N} \sum_{n=0}^{N-1} \sum_{m=0}^{N-1} r(n) c(m) \sum_{k=0}^{N-1} e^{i2\pi k(m-n+j)/N}$$
$$= \frac{1}{N} \sum_{n=0}^{N-1} r(n) c(n-j)$$

Equation 7

Based on Fast Fourier Transform, the circular correlation consists in evaluating the autocorrelation function for all the code delays and for one Doppler frequency. This process is repeated for all Doppler frequencies in the frequency search space. This method is largely described in [Al Bitar, 2007] and [Fantino et al., 2008] for example. It reduces greatly the number of operations and does not degrade the quality of the correlation. This acquisition method is the Reference Acquisition to which we will compare our method. It is an optimized variant of the classical acquisition although the autocorrelation function is computed on large size vectors.

There are several acquisition methods which exploit the circular correlation, to name a few: coherent integration by summing before/after IFFT-FFT [Al Bitar, 2007], half sized circular correlation [Lin & Tsui, 1998]. The goal of these techniques is always to reduce the computation time (by reducing the size of vectors or the number of operations) and enhance sensitivity. The acquisition step requiring a lot of time and operations, there are many developed techniques, some of them are not based on the circular correlation, such as Delay and Multiply method [Tsui, 2004] and Multi-C/A method [Lin & Jan, 2007].
Another method is the Double Block Zero Padding (DBZP), which is discussed in [Chibout, 2008], [Lin et al., 1999]. [Ziedan, 2006], developed also a Modified DBZP (MDBZP) to foil the Doppler frequency effect on the code frequency. [Lin & Tsui, 2000] compared 8 of the previously cited acquisition methods and concluded that the DBZP seems to be one of the best for the acquisition of weak signals due to the reduced number of operations. [Chibout, 2008] confirmed this result by comparing the DBZP with two others acquisition methods (1+1ms FFT method described later and Half bit method) and concluded that the DBZP acquisition method requires 200 times fewer calculations and run more than 20 times faster than the two other methods. This is why the DBZP is found as a relevant method to be used as a base for developing a new Galileo E1 OS acquisition technique.

Galileo E1 OS acquisition methods

The acquisition of Galileo E1 OS signals is very different from that of GPS L1 C/A due to its significantly different structure, as reminded in Table 1.

Let's notice that the Galileo E1 OS autocorrelation functions also include the subcarrier (the example with the data spreading code is given here):

$$R_{c_{1,D}}(m)$$
$$= \frac{1}{4092} \sum_{l=0}^{4092-1} c_{1,D}(l) p_{CBOC,D}(l) c_{1,D}(l-m) p_{CBOC,D}(l-m)$$

Equation 8

where:

- $c_{1,D}$ and $c_{1,P}$ are the spreading sequences carried by the data and pilot components

- $R_{c_{1,D}}$ and $R_{c_{1,P}}$ are the autocorrelation functions of the data and pilot spreading codes

Let's notice that the Galileo E1 OS autocorrelation function (which can be approximated by a BOC(1,1) autocorrelation function in red in Figure 2) peak is narrower than GPS L1 C/A (in blue dotted line) one and this leads to a thinner discretization in time for the acquisition of Galileo E1 OS signal.

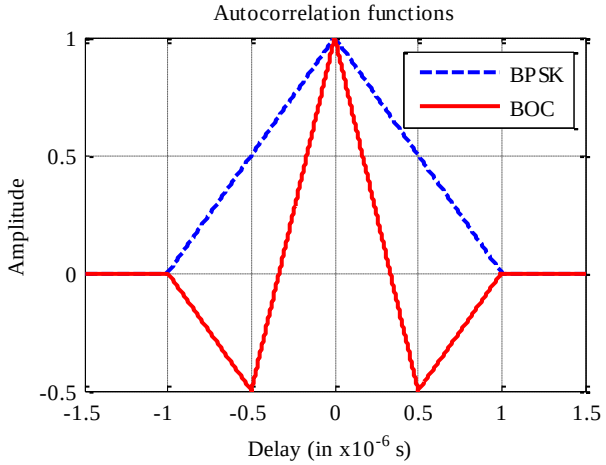

Figure 2 – Correlation peaks for GPS L1 C/A (BPSK) and Galileo E1 OS signals (BOC)

There are several techniques that have been proposed to acquire Galileo E1 OS signal.

One solution to acquire Galileo E1 OS signal consists in ignoring the data component and only acquire the pilot component (because it is modulated by a known secondary code contrary to the data component which is modulated by the unknown navigation message). In this way, only half of the useful power is employed. This method is not adapted to the acquisition of weak signals. Another one, developed by [Corazza et al., 2006], only acquires the pilot component and constructs a secondary code evolutionary tree to handle the secondary code ambiguity by enumerating all possible sign combinations of the 25 consecutive secondary code chips, leading to process 25 outputs. This acquisition method needs a considerable memory capacity to store the transient values.

The pilot and data component can also be combined to allow recovering all the available power improving the acquisition performance. There are several acquisition strategies to combine the two components.

- The first one (called non-coherent combining in [Borio & Lo Presti, 2008] and joint acquisition in [Pajala et al., 2005]) considers separately the two components. The received signal is correlated separately with the local codes of the data and pilot components. The correlation outputs are then squared and summed. For example, [Bastide et al., 2002] studied the performance of this method applied to L5/E5 signals in terms of false alarm and detection probabilities.
- The second one (which shows more interesting properties than the previous ones) performs the correlation on a complete period of the secondary code to fully exploit its capability and significantly increase the sensibility by finding the secondary code phase at the same time. The down-converted received signal is multiplied with a delayed primary code and complex carrier replicas. Then, the obtained mixing results are added over a spreading code period. The integration and dump over one spreading code period is repeated 25 times for the same code phase and frequency bin. The secondary code still lies under the obtained signal and in order to find it, a parallel code phase acquisition is performed. The development of this algorithm is given in [Tawk et al., 2011]. This FFT-based algorithm allows reaching a good sensitivity, all of this with a reasonable complexity.
- The last one is the coherent combining with sign recovery which is developed in [Borio & Lo Presti, 2008]. The incoming signal is correlated simultaneously with two code equivalent sequences and the decision variable is obtained by choosing the maximum of the two correlation outputs. It is presented by the Figure 3 where the two code equivalent sequences are the sum and the difference of the spreading codes. In this way, the computational load is similar to the non-coherent combining acquisition method. Nonetheless, this acquisition method outperforms due to its effectiveness (performance degradation of coherent combining for low C/N_0) [Borio & Lo Presti, 2008].

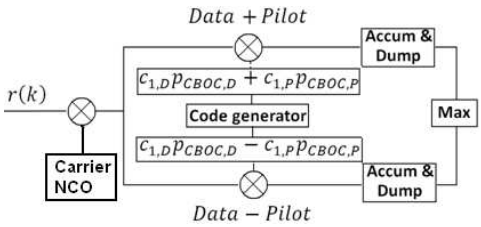

Figure 3 - Acquisition strategy for Galileo E1 OS signal

The acquisition strategy for Galileo weak signals is to collect the total power of the incoming signal by combining the two components. Let's evaluate the result of the multiplication of the incoming signal by the two code equivalent sequences (the sum and the difference of the two spreading codes including the subcarriers) and noted by the parameter α:

$$\begin{aligned}&\left(d(k)c_{1,D}(k)p_{BOC,D}(k) - c_2(k)c_{1,P}(k)p_{BOC,P}(k)\right)\\&\times\left(c_{1,D}(k)p_{BOC,D}(k) + \alpha c_{1,P}(k)p_{BOC,P}(k)\right)\\&= d(k)R_{c_{1,D}}(k) - \alpha c_2(k)R_{c_{1,P}}(k)\\&+\left(\alpha d(k) - c_2(k)\right)R_{c_{1,D/P}}(k)\end{aligned}$$

Equation 9

where

- $\alpha = \pm 1$ is the parameter to distinguish the two equivalent code sequences
- $R_{c_{1,D}}$ and $R_{c_{1,P}}$ are the autocorrelation functions of the two spreading codes (data and pilot) for the same satellite
- $R_{c_{1,D/P}}$ is the cross-correlation function between the two spreading codes

Thus, a necessary condition to maximize the criterion is $d(k) = -\alpha c_2(k)$. The Table 2 in Appendix A evaluates all data and secondary code bit combinations and gives the code equivalent sequence. As we can see in Figure 4, only one of the two code equivalent sequences represents the correlation with the incoming signal, the other is should be dominated by noise.

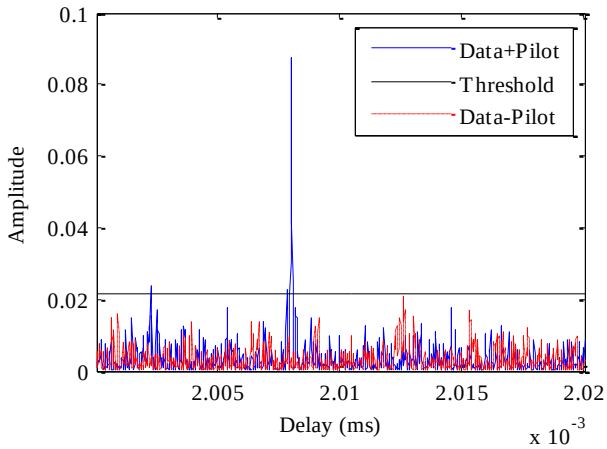

Figure 4 - Correlation with the 2 equivalent code sequences

The choice of the memory codes for Galileo E1 OS is such as $R_{c_{1,D}/c_{1,P}}$ is negligible [Wallner et al., 2007]. Without loss of generality, let's note $R(\varepsilon_\tau(k)) = R_{c_{1,D}}(\varepsilon_\tau(k)) + R_{c_{1,P}}(\varepsilon_\tau(k))$ which takes 2 as maximal value.

The performance of the Galileo E1 OS coherent combining acquisition method rests among other on the local code generation (two code equivalent sequences). It is why for the DBZP and its variant applied to Galileo E1 OS signal, the local code generation consists in the generation of the sum and difference of the two spreading codes.

In this first part, a review of structure of the GPS L1 C/A and Galileo E1 OS signals is proposed as well as a state of the art of the acquisition methods of these two signals. It highlights a computationally efficient acquisition method which is well suited for the acquisition of weak GPS L1 C/A signals. In the following part, the Double Block Zero Padding is described as well as its mathematical model.

II. DBZP ACQUISITION METHOD

As seen previously, the classical acquisition methods compute a 2D acquisition matrix in order to find the right delay and the right Doppler frequency which affects the signal by minimizing the code delay error and the Doppler frequency error. In the Double Block Zero Padding (DBZP) method, the delay/Doppler research is not achieved following that kind of time/frequency research, using a 2D acquisition matrix. The code delay follows the same search scheme but in the DBZP, we directly search the incoming Doppler frequency without generating a local carrier including a Doppler frequency estimated.

The concept of the DBZP relies on the use of partial correlations on a duration equivalent to a few tens of chips and an extensive use of Fourier transforms to compute these partial correlations. To do so, the incoming signal and the local code are split into blocks, one pair of blocks for one partial correlation. The computation time gain of the DBZP is the FFT processing on small size vectors instead of large size vectors (as for Reference Acquisition).
Figure 5 presents a new DBZP scheme.

DBZP mathematical model

In this part, the general mathematical model of the DBZP technique is analyzed. The DBZP is described in 5 steps.

Parameters

First of all, let's define the parameters of the DBZP technique. The user defines 2 parameters:

- t_i is the desired coherent integration time
- $[-f_{Max}; f_{Max}]$ is the Doppler frequency interval where f_{Max} is the maximal expected value of the incoming Doppler frequency

The deduced inputs of the algorithms are:

- $M = \frac{2f_{Max}}{\frac{1}{t_i}} = 2f_{Max} \times t_i$ is the number of blocks in which the incoming signal is split over t_i. It depends on the integration time and on the width of the Doppler frequency interval
- $t_{block} = \frac{t_i}{M} = \frac{1}{2f_{Max}}$ is the duration of one block
- *N* is the number of samples per block

Description of the DBZP algorithm

- *Step 1: Pre-processing of the incoming signal*

First, t_i ms of the incoming signal are converted into baseband by multiplying it by a complex subcarrier:

$$r(t) \times exp(-i2\pi f_{IF} t)$$

So the incoming signal in baseband is complex.

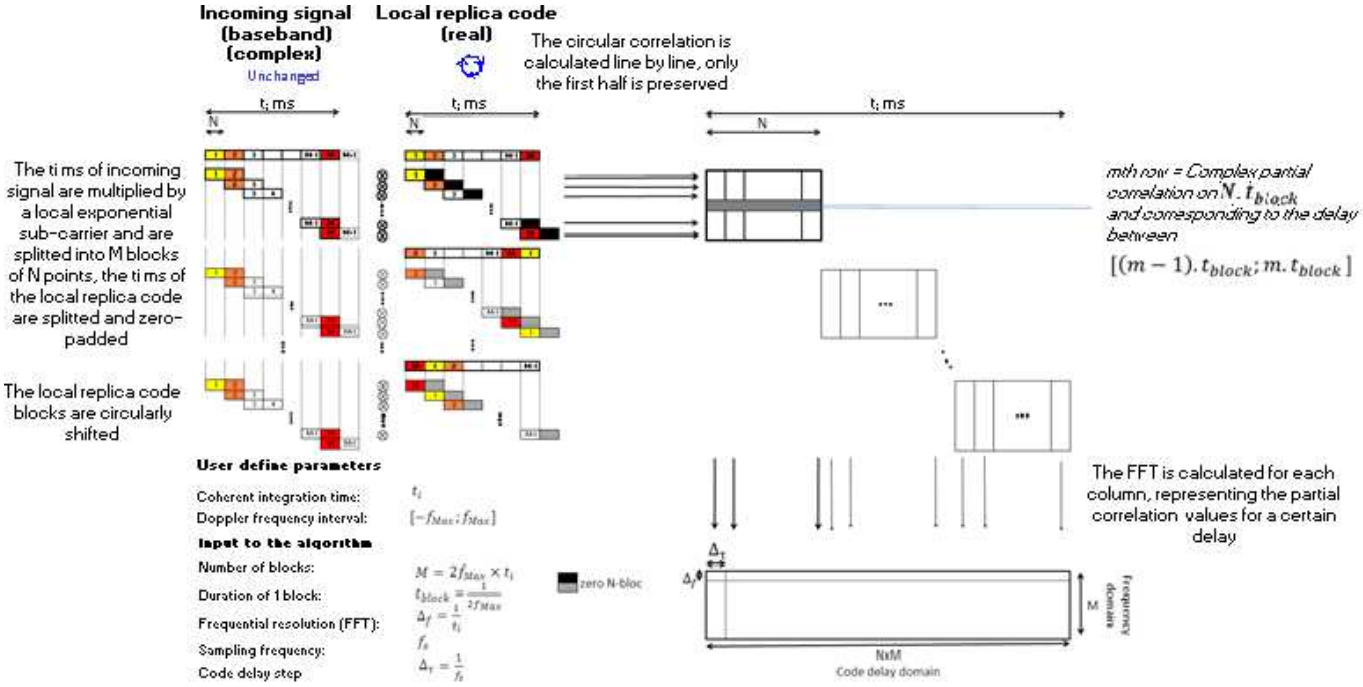

Figure 5 - DBZP scheme

Then, the samples are split into M blocks of equal length. Each block contains the same number of samples (N).
After that, each two adjacent blocks of the received signal are combined to form a block of $2N$ samples (thus the name "Double Block"). The last block is combined with additional samples.
Notice that when the number of received samples is not divisible by the number of blocks, the number of samples is then adjusted (by adding or removing samples) such that the number of samples divided by the number of blocks is an integer.

It is important to understand that the local exponential carrier does not try to compensate the incoming Doppler frequency as it is the case for the other acquisition methods.

- *Step 2: Local replica code*

t_i ms of the local replica spreading code are generated and arranged into the same number of blocks (that have the same length) as the incoming signal. Each block is zero-padded, this means that N samples of value 0 are appended to each block, as we can see in the
Figure 5 where the zero N-block is represented by a black box.

- *Step 3: Partial circular correlation*

The first 2N-sample block of incoming signal is circularly correlated with the first zero-padded code block of the local replica and only the first half of the resulting correlation function is preserved. The circular correlation using FFTs is done for all M pairs of blocks. The N points represent a partial correlation of length t_i/M ms (which is much shorter than a spreading code period) at N possible code delays.

For this step, there are two important points to understand:

- The reason why the size of the blocks used for the circular correlation is extended by combining two adjacent data blocks for the incoming signal and by zero-padding the code block for the local signal
- What does a partial correlation represent?

To compute the circular correlation, the same principle as the "1+1 ms FFT acquisition method" [Chibout, 2008] is in fact used by the DBZP. The "1+1 ms" technique is a GPS L1 C/A signal acquisition method. 2 ms of the incoming signal is stored in a data buffer. Besides, a 1-ms local code replica is 1-ms-zero-padded. A circular correlation is then computed between these two extended blocks and only the first half is kept to represent only code delays between 0 and 1 ms. This technique is efficient in avoiding the correlation losses due to data bit transition that can occur inside the first 1 ms of the data block. In conclusion, the result of this circular correlation is equivalent to a correlation on 1 ms where no data transition bit occurs.

In the DBZP, the principle of the "1+1 ms" acquisition method is kept with the difference that it is applied on partial correlation. It thus avoids losses due to possible data bit transition (inside a partial correlation).

Incidentally, it is also necessary to use this trick to go over the non-periodicity of the partial code blocks as illustrated in Figure 6.

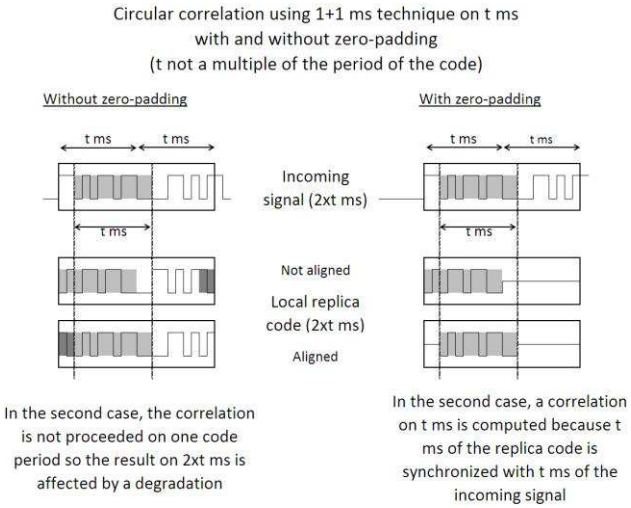

Figure 6 - Circular correlation using 1+1 ms technique

The second point to discuss is the advantages and drawbacks of using partial correlation instead of the full correlation. The normalized partial autocorrelation function is equivalent to the normalized full autocorrelation function in the neighborhood of the right code delay (below 1 chip). The drawback being that the correlation is done only a part of the whole spreading code and thus the properties of the spreading code are not kept. As a consequence, the isolation of the main peak with respect to the secondary peak will be much lower. This is highlighted by Figure 7. The figure on the right represents the partial and full autocorrelation for one Galileo spreading code (data or pilot).

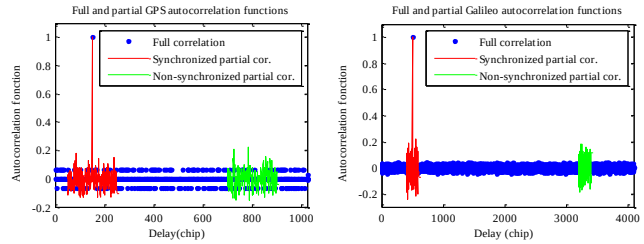

Figure 7 - Full and partial GPS L1 C/A PRN and Galileo E1 OS code autocorrelation functions

Mathematically, the expressions of the real and imaginary parts of the partial correlation outputs are given (the details can be found in Appendix E):

$$\widetilde{I_p}(l,k) = n_{\widetilde{I_p}}(l,k) + \frac{A}{2}R_p(\varepsilon_\tau(k))sinc\left(\frac{\pi t_i}{M}f_D\right)cos\left(2\pi f_D\left(t_0+\frac{lt_i}{M}+\frac{t_i}{2M}\right)+\varepsilon_{\phi_0}\right)$$

$$\widetilde{Q_p}(l,k) = n_{\widetilde{Q_p}}(l,k) + \frac{A}{2}R_p(\varepsilon_\tau(k))sinc\left(\pi f_D\frac{t_i}{M}\right)sin\left(2\pi f_D\left(t_0+\frac{lt_i}{M}+\frac{t_i}{2M}\right)+\varepsilon_{\phi_0}\right)$$

Equation 10

where

- $l = 1 \dots M$ stands for the l^{th} partial correlation
- $k = 1 \dots N$ stands for the k^{th} sample
- $\varepsilon_\tau(k)$ represents the delay associated to the k^{th} sample
- $\widetilde{I_p}(l,k)$ and $\widetilde{Q_p}(l,k)$ are the in-phase and quadrature l^{th} partial correlator outputs for the error on the code delay $\varepsilon_\tau(k)$
- R_p is the partial correlation
- $n_{\widetilde{I_p}}$ and $n_{\widetilde{Q_p}}$ are the noise for the two correlator outputs and of variance:

$$\sigma^2_{\widetilde{I_p}} = \sigma^2_{\widetilde{Q_p}} = 2 \times \frac{N_0}{4\frac{t_i}{M}}$$

Equation 11

The partial correlator outputs can be stored in a matrix where each column represents a code delay ($\varepsilon_\tau(k)$) and each row contains the partial correlation function for all code delays (M rows for M partial circular correlations).

The phase of the cosine term (in Eq. 10) depends on the slice of time of the partial correlation (through l) and on the incoming Doppler frequency f_D (and not on the error on the Doppler frequency as it is the case for the Reference Acquisition method). So if a FFT is applied on this term, the incoming Doppler frequency can be easily determined.

- *Step 4: Application of the FFT*

A M-point Fourier transform is applied to the set of partial correlation outputs corresponding to a given code delay. The process is repeated for all the possible code delays so, N M-point FFT's are performed, as we can see in the Figure 5.

It can be assumed that $\frac{A}{2}R_p(\varepsilon_\tau(k))sinc\left(\frac{\pi t_i}{M}f_D\right)$ is constant for all l in $[\![1;M]\!]$ and approximated by $\frac{A}{2}R(\varepsilon_\tau(k))sinc\left(\frac{\pi t_i}{M}f_D\right)$ for the right code delay. So, let's compute the FFT of the cosine/sine term in $\widetilde{I_p}(l,k)$ and $\widetilde{Q_p}(l,k)$ by applying the Euler form and using the result of Appendix B:

$$FFT\left(cos\left(2\pi f_D\left(t_0+\frac{lt_i}{M}+\frac{t_i}{2M}\right)+\varepsilon_{\phi_0}\right)\right)(m_{m=0\dots M-1})$$

$$= \sum_{l=0}^{M-1} cos\left(2\pi f_D\left(t_0+\frac{lt_i}{M}+\frac{t_i}{2M}\right)+\varepsilon_{\phi_0}\right)e^{-\frac{i2\pi ml}{M}}$$

$$= \frac{M}{2}e^{i\left(\left(2\pi f_D\left(t_0+\frac{t_i}{2M}\right)+\varepsilon_{\phi_0}\right)-\pi\frac{(M-1)}{M}(m-f_Dt_i)\right)}\frac{\text{sinc}(\pi(m-f_Dt_i))}{\text{sinc}\left(\frac{\pi(m-f_Dt_i)}{M}\right)}$$

$$+ \frac{M}{2}e^{i\left(\left(2\pi f_D\left(t_0+\frac{t_i}{2M}\right)+\varepsilon_{\phi_0}\right)-\pi\frac{(M-1)}{M}(m+f_Dt_i)\right)}\frac{\text{sinc}(\pi(m+f_Dt_i))}{\text{sinc}\left(\frac{\pi(m+f_Dt_i)}{M}\right)}$$

Equation 12

where

- m is the point where the FFT is taken

$$\iota(k) = FFT\left(\widetilde{I_p}\right)$$

$$= \frac{A}{4} MR(\varepsilon_\tau(k)) sinc\left(\frac{\pi t_i}{M} f_D\right) e^{-\frac{i\pi(M-1)}{M}m} \left(e^{i(\pi f_D(2t_0+t_i)+\varepsilon_{\phi_0})} \frac{\text{sinc}(\pi(m - f_D t_i))}{\text{sinc}\left(\frac{\pi(m - f_D t_i)}{M}\right)} + e^{-i(\pi f_D(2t_0+t_i)+\varepsilon_{\phi_0})} \frac{\text{sinc}(\pi(m + f_D t_i))}{\text{sinc}\left(\frac{\pi(m + f_D t_i)}{M}\right)} \right) + n_\iota(k)$$

$$\rho(k) = FFT\left(\widetilde{Q_p}\right)$$

$$= -i \times \frac{A}{4} MR(\varepsilon_\tau(k)) sinc\left(\frac{\pi t_i}{M} f_D\right) e^{-\frac{i\pi(M-1)}{M}m} \left(e^{i(\pi f_D(2t_0+t_i)+\varepsilon_{\phi_0})} \frac{\text{sinc}(\pi(m - f_D t_i))}{\text{sinc}\left(\frac{\pi(m - f_D t_i)}{M}\right)} - e^{-i(\pi f_D(2t_0+t_i)+\varepsilon_{\phi_0})} \frac{\text{sinc}(\pi(m + f_D t_i))}{\text{sinc}\left(\frac{\pi(m + f_D t_i)}{M}\right)} \right) + n_\rho(k)$$

Equation 13

At the end, the two complex outputs of the DBZP are given by the Eq. 13 where $\iota(k), \rho(k), n_\iota(k), n_\rho(k)$ are complex.

The frequential resolution for the FFT is $\Delta_f = \frac{1}{t_i}$, the code delay resolution is $\Delta_\tau = \frac{1}{f_s}$ where f_s is the sampling frequency.

- *Step 5: Permutation of the code blocks*

In the process previously described, only code delays in the interval $\left[0; \frac{t_i}{M}\right[$ ms can be tested. To test the other code delays, the local spreading code blocks are circularly permutated: the M^{th} block becomes the first, the first becomes the second, etc… M permutations like this can be done in order to test all the code delays.

For example, for the GPS L1 C/A, [Lin et al., 1999], the Doppler frequency interval is $[-10\,kHZ; 10kHz]$ and $t_i = 10\,ms$. This leads to $M = 200$ blocks. The duration of one block is independent from the coherent integration time t_i and for a Doppler frequency interval of length 20 kHz, the duration of one block t_{block} is $0.05\,ms$. The frequential resolution is $\Delta_f = 100\,Hz$.

Comparison of the Reference and DBZP acquisition methods

This section deals with the comparison of the two acquisition methods: the DBZP and the Reference Acquisition (RA) on 3 points.

- *Number of operations*

The DBZP is exclusively based on the use of FFTs on small-sized blocks. If the size of the blocks (N), can be expressed as a power of 2, there are optimized FFT algorithms as the Rooley-Tukey algorithm which speed up the computation time of the operation and its complexity is in $\mathcal{O}(Nlog(N))$. The number of multiplications is $\frac{N}{2}\log_{10}(N)$ and the number of addition is $N\log_{10}(N)$. But in the naive way (when N is not a power of 2), the complexity is in $\mathcal{O}(N^2)$. Still, by means of zero-padding or truncation, it is possible to force the size of vector to the nearest or next power of 2, whichever the original size.

The following parameters were chosen for Matlab simulations and theoretical computation results:

- Sampling frequency: $f_s = 20.48\,MHz$,
- Integration time: $t_i = 4\,ms$ (for Galileo 1 OS processing)
- Doppler uncertainty: $f_D \in [-10; 10]\,kHz$

Let's compare the number of operations with the DBZP and Reference Acquisition methods. The number of incoming signal samples is 81920.

DBZP:

- Number of points per blocks, not double sized: $N = 1024$
- Number of blocks: $M = 80$

Reference Acquisition:

Number of Doppler bins: $\frac{20000}{\frac{1}{2t_i}} = 161$

The number of elementary operations (additions and multiplications) is evaluated for the two acquisitions methods. We give the details in Appendix G but the main result is that for one acquisition, there are 2.2 times less elementary operations for the DBZP algorithm in regard with the Reference Acquisition. Indeed, there are $1.3e^8$ operations for the DBZP algorithm and $2.7e^8$ for the Reference Acquisition, these numbers are obtained with optimized FFT algorithm.

The computationally efficiency of the DBZP is confirmed with the estimation of the number of CPU cycles which is lower (divided by 2.4) in the case of DBZP algorithm.

The computation time of the DBZP divides by 2.6 the computation time of the Reference Acquisition (123 seconds instead of 320 seconds for Matlab simulations).

The DBZP is thus very interesting to optimize the computational burden of the acquisition process. This justifies the choice of this acquisition method for the acquisition of Galileo E1 OS signal.

- *Signal to Noise Ratio*

To study the performance of DBZP, the Signal-to-Noise-Ratio (SNR) at the DBZP output needs to be analyzed. The power of the noise at the partial correlation output is:

$$\sigma^2_{\widetilde{I_p}} = \sigma^2_{\widetilde{Q_p}} = 2 \times \frac{N_0}{4\frac{t_i}{M}}$$

So, by taking the FFT of the M partial correlation outputs, the power of the noise at the DBPZ output is:

$$P_{n_I} = P_{n_Q} = M \times 2\frac{N_0}{4\frac{t_i}{M}} = \frac{M^2 N_0}{2t_i}$$

Equation 14

Let's compute the power of the useful signal at the DBZP output, assuming that the local code replica is perfectly synchronized with the incoming signal:

$$P_s = I^2(k) + Q^2(k)$$

$$= \left(\frac{A}{2}MR\left(\varepsilon_\tau(k)\right)sinc\left(\frac{\pi t_i}{M}f_D\right)\frac{\text{sinc}(\pi(m - f_D t_i)\,)}{\text{sinc}\left(\frac{\pi(m - f_D t_i)}{M}\right)}\right)^2$$

$$\leq \frac{A^2}{4}M^2 \times R^2\left(\varepsilon_\tau(k)\right)$$

Equation 15

Then, the SNR is:

$$\frac{P_s}{P_{n_I}} = \frac{A^2M^2}{\frac{M^2N_0R^2\left(\varepsilon_\tau(k)\right)}{2t_i}} = \frac{A^2 t_i R^2\left(\varepsilon_\tau(k)\right)}{2N_0} = 2\frac{P}{N_0}t_i$$

Equation 16

The SNR at the correlator output for the Reference Acquisition and for the DBZP output are the same (given in [Julien, 2008] for the Reference Acquisition) which means that the two acquisition algorithms are equivalent in terms of SNR.

- *Width of the peak*

In the frequency domain, the width of the main peak (for the right code delay and for the right incoming Doppler frequency) is the same for the two acquisition methods as we can see in Figure 8 and it is $1/2t_i$ although it does not have the same signification.

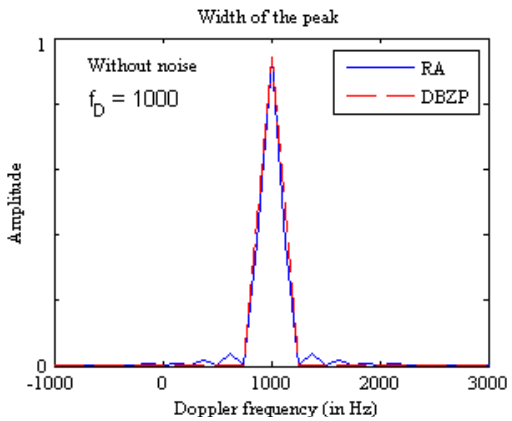

Figure 8 - Width of the peak for the two acquisition methods

The DBZP output can be assimilated as a Dirac function (or a weighted sum of two Dirac functions for frequencies which are not a multiple of $1/t_i$) and the width of the peak corresponds to the interval of the first zeros bordering the main peak, that means $2 \times 1/t_i$.

For the Reference Acquisition method, the width of the peak is given by the width of the main peak of $sinc\left(\pi\varepsilon_{f_D}t_i\right)$ which is $2 \times 1/t_i$. We refer to the reader interesting by the Reference Acquisition criterion to the exhaustive list of papers about this, for example [Borre et al., 2007].

After a theoretical comparison of the two acquisition methods, it was seen that the DBZP presents better results in terms of computation efficiency without adding noise. The noise level is the same for the two acquisition methods and the width of the main peak is the same for both acquisition methods. Then, the DBZP speeds up the acquisition without degrading the performance.

DBZP Acquisition Criterion

The expression of the criterion is (using Eq. 13):

$$|\iota(k) + i\rho(k)|^2$$

$$= \left(\mathcal{R}\left(\iota(k)\right) - Im(\rho(k))\right)^2 + \left(\mathcal{R}\left(\rho(k)\right) + Im\left(\iota(k)\right)\right)^2$$

$$= I(k)^2 + Q(k)^2$$

$$= \left(\frac{A}{2}MR\left(\varepsilon_\tau(k)\right)sinc\left(\frac{\pi t_i}{M}f_D\right)\frac{\text{sinc}(\pi(m - f_D t_i)\,)}{\text{sinc}\left(\frac{\pi(m - f_D t_i)}{M}\right)}\right)^2$$

$$+ n_I^2(k) + n_Q^2(k)$$

Equation 17

The acquisition criterion is then:

$$T = \sum_{k=1}^{K}\left(I^2(k) + Q^2(k)\right)$$

where

- K is called the non-coherent integration number
- $m = 1 \ldots M$ is the index on the Doppler frequency bins

The acquisition criterion takes into account the two components (data and pilot), let's remind that the local code is the sum and the difference of the spreading codes on the two components.

Limitations of the DBZP

- *Dependence on the incoming Doppler frequency*

The useful part of the DBZP acquisition criterion (see Eq.17) has 2 parameters that depend on the incoming Doppler frequency f_D which is very unusual compared to classical acquisition scheme. This is mostly due to the fact that only 1 local replica is generated to compute the whole acquisition grid.

First, the amplitude of $sinc\left(\frac{\pi t_i}{M}f_D\right)$ entails a degradation of the amplitude of the useful part of the criterion for high values of the incoming Doppler frequency (in absolute value) which leads to a maximum loss of 4 dB as we can see in Figure 9.

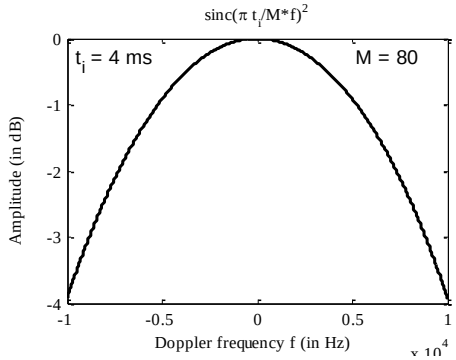

Figure 9 - Degradations of the criterion for high frequencies

Let's note that:

$$\frac{t_i}{M} f_D = \frac{t_i}{2 t_i f_{Max}} f_D = \frac{1}{2} \frac{f_D}{f_{Max}}$$

So, these degradations depend on the Doppler frequency interval through the maximal expected value of the incoming Doppler frequency.

Secondly, the ratio of $sinc$ in Eq. 17 depends on the value of $m - f_D t_i$ where m is the FFT index and m within $[\![1; M]\!]$. If $m - f_D t_i$ is an integer, which is equivalent to f_D being a multiple of $1/t_i$, then it is exactly a Dirac function:

$$\frac{\mathrm{sinc}(\pi(m - f_D t_i))}{\mathrm{sinc}\left(\frac{\pi(m - f_D t_i)}{M}\right)} = \delta_0(m - f_D t_i)$$

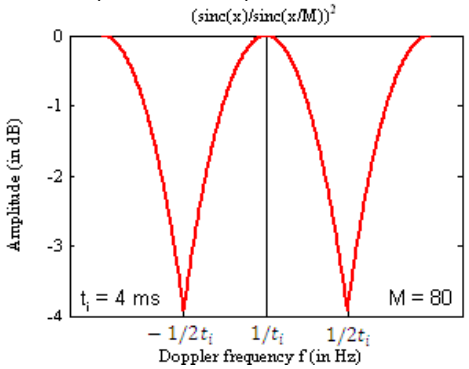

Figure 10 - Behaviour of the ratio of sinc

In the other cases (when f_D is not a multiple of $1/t_i$), $\frac{\mathrm{sinc}(\pi(m - f_D t_i))}{\mathrm{sinc}\left(\frac{\pi(m - f_D t_i)}{M}\right)}$ is equivalent to a weighted sum of Dirac. In the worst case, if f_D is exactly between two multiples of $1/t_i$ $\left(f_D = \left(k + \frac{1}{2}\right)\frac{1}{t_i}, k \in [\![-M; M]\!]\right)$ the main peak is divided into 2 subpeaks of a reduced amplitude and this implies a maximum degradation of 4 dB (Figure 10).

Based on this discussion, Figure 11 represents the overall power loss due to the incoming signal Doppler frequency.

The conclusion on the criterion is that its amplitude has a strong dependence on the incoming Doppler frequency, which is the counter part of using only a single local replica for the whole acquisition grid. In particular, its amplitude can be greatly reduced for Doppler frequencies between two multiples of $1/t_i$ and for high Doppler frequencies. It is very important to highlight that this inherent drawback of the DBZP has never been reported in the literature to the authors' knowledge.

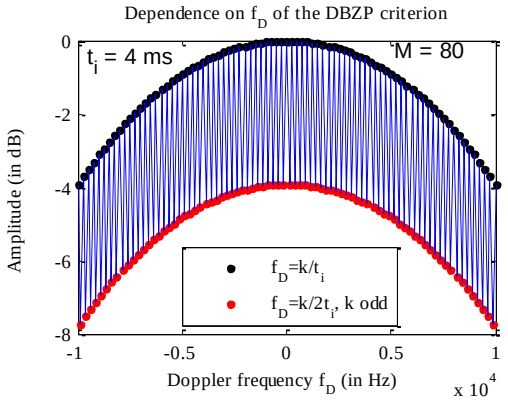

Figure 11 - Amplitude of the criterion versus the incoming Doppler frequency

- *Bit transition sensitivity*

The presence of a bit transition has a huge impact on the behavior of the criterion. It decreases the power of the criterion until to be null if the transition occurs in the middle of the integration period (as we can see in Figure 12) and thus, due to the presence of others peaks, the estimation of the incoming Doppler frequency can be distorted.

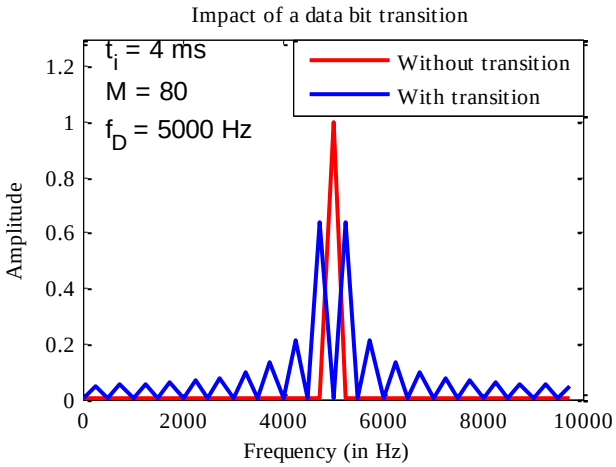

Figure 12 - Impact of a data bit transition

It is possible to show that the presence of a bit transition does not completely cancel the probability of detection, depending on the location of the transition within the correlation period. It can also be shown that it can introduce an error in the selection of the estimated parameters (Doppler frequency) [Sun & Lo Presti, 2010] as the bit transition can be interpreted as a sub-carrier.
In Appendix F, the details of the computation of the Fast Fourier Transform of the following expression (applying to the DBZP) is given:

$$d(l)\cos\left(2\pi f_D\left(t_0 + \frac{l t_i}{M} + \frac{t_i}{2M}\right) + \varepsilon_{\phi_0}\right)$$

It permits to mathematically understand what happens when we apply a FFT on a vector where the data bit ($d(l)$) is not the same for all elements (partial correlation outputs). The degradations of a data transition can be explained by the decomposition of $Me^{-i\pi\frac{(M-1)}{M}(m-f_D t_i)}$ into 2 exponential terms:

$$-Le^{-i\pi\frac{(L-1)}{M}(m-f_D t_i)} + (M-L)e^{-i\pi\frac{(M-L-1)}{M}(m-f_D t_i)}$$

where

- $L \in [\![1, M]\!]$ represents the time when the data bit transition occurs

The representation of the DBZP criterion with and without data transition is given in Figure 13.

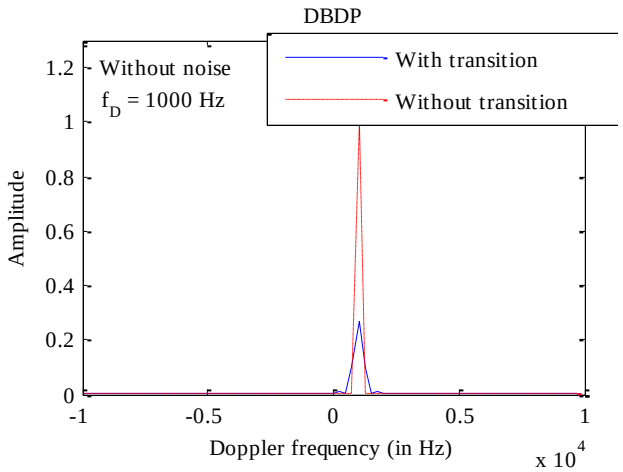

Figure 13 - Impact of a data bit transition on the DBZP criterion

The presence of a data bit sign transition completely destroys the code periodicity so leading to serious impairments. In the case of GPS L1 C/A, a data bit transition can occur at the maximum every 20 ms but in the case of Galileo E1 OS, a data bit transition (and secondary code bit transition) can occur every 4 ms. As a consequence, since there is no synchronization with the incoming signal during the acquisition process, it is likely that a bit transition occur during the correlation period (more or less 50% chance). The short Galileo data bit duration makes the acquisition of Galileo E1 OS more sensitive to transition and it appears important to solve for this sensitivity when design a Galileo E1 OS signal acquisition method.

III. DBZPTI ACQUISITION METHOD

To be resistant to the effect of data bit transition on the Galileo E1 OS acquisition technique, a Galileo E1 OS acquisition technique, the Double Block Zero Padding Transition Insensitive (DBZPTI) is proposed. The parameters and the four first steps of the DBZP described earlier are kept the same. However, the bit transition resistance is possible with the fifth following step.

- *Step 5': Shift of the incoming signal blocks*

Instead of circularly permutating the blocks of the local code to simulate all possible code delays, it is the incoming signal that is time-shifted by one block in a linear way (this means 2 t_i ms of incoming signal are used). Thereby, if the coherent integration time is one code period, the DBZPTI output for the right delay has to be done on a code period without data (and secondary code) bit.

Indeed, the acquisition process consists in finding the beginning of a spreading code period (in the case of Galileo E1 OS acquisition, it means also when a data bit

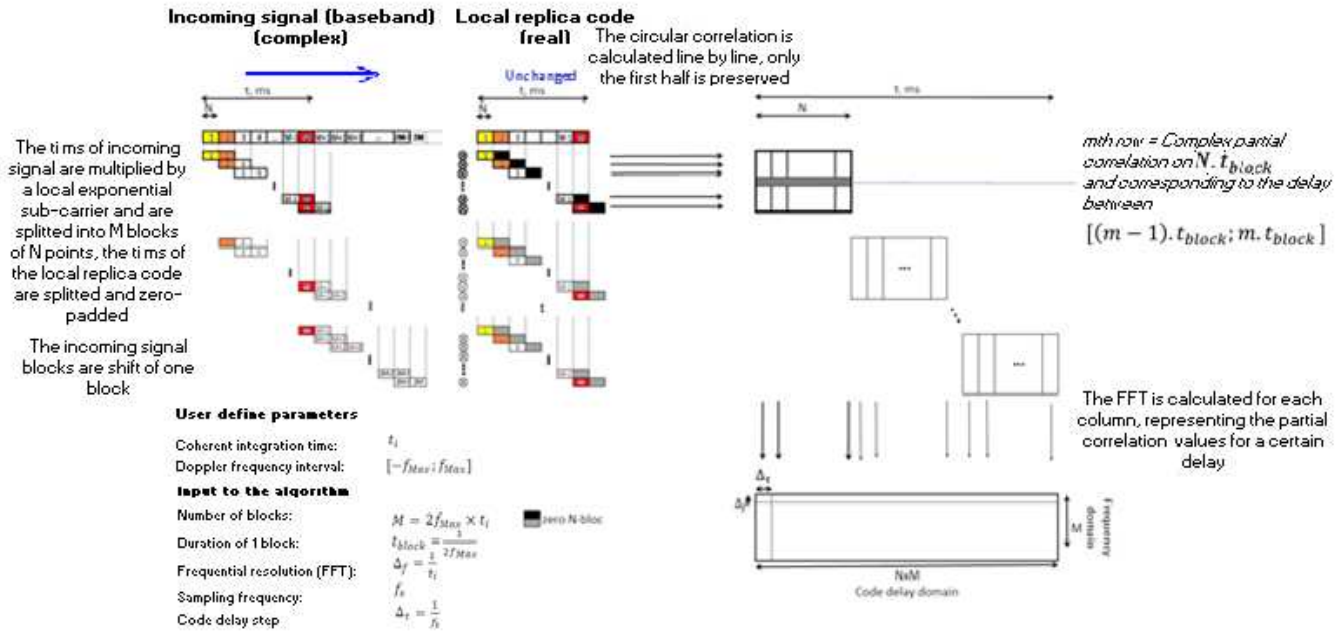

Figure 14 - DBZPTI scheme

or secondary code bit occurs). As can be seen in Figure 15, if a data transition occurs during the integration time, the incoming code and the local code are properly aligned for the DBZP but there is a transition. However, for the DBZPTI, it is the principle of a sliding windows of length t_i ms (the length of a data bit). Differently from the "1+1ms" described earlier, this method has the advantage to compute correlation output on the duration of one code period and not over two code periods.

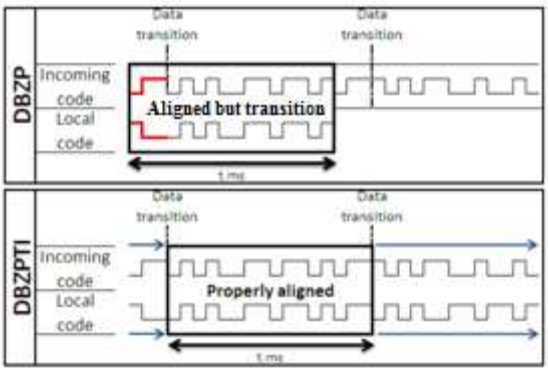

Figure 15 - DBZPTI principle

At the end, the general scheme of the DBZPTI is given by the Figure 14 which differs only in the fifth step from the Figure 5.

It was checked using simulations that there is no degradation in the DBZPTI acquisition criterion amplitude. The result is presented in Figure 16. The amplitude of the DBZPTI criterion is the same with or without transition in the incoming signal. The blue curve fits the shape of the red curve.

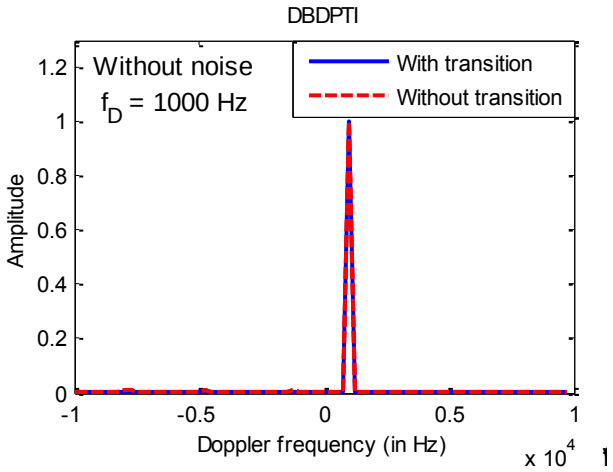

Figure 16 - DBZPTI criterion with/without transition

On the contrary, if there is a transition (Figure 17), there are important degradations (at the maximum 6 dB, if the transition exactly occurs in the middle of the integration time) in the amplitude of the Reference Acquisition criterion and the acquisition cannot be on the right Doppler frequency (as it is explained previously and represented by Figure 12).

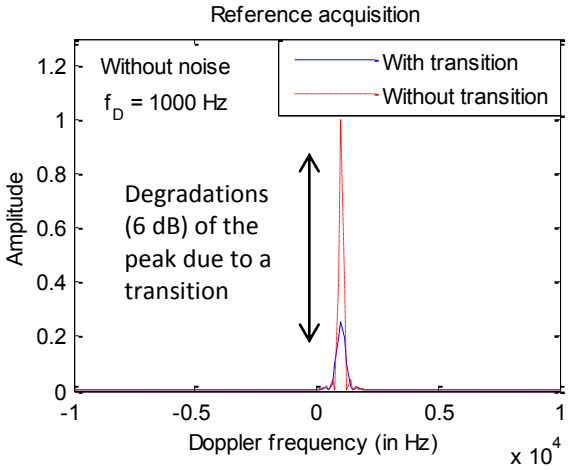

Figure 17 - Reference Acquisition criterion with/without transition

To summarize, the DBZPTI presents the same features that the DBZP and previously showed:

- This acquisition method is computationally efficient. In the case of the DBZPTI, $2t_i$ ms of incoming signal is processed but the number of operations does not change
- The noise level of the DBZPTI is comparable to other acquisition methods (Reference Acquisition and DBZP)
- The performance unfortunately strongly depends on the incoming Doppler frequency

However, the DBZPTI is transition insensitive if t_i is chosen equal to a data (or secondary code) bit duration that means 4 ms.

Let's note that, for the DBZP and DBZPTI, the Galileo local code generation consists in the generation of the sum and the difference of the two spreading codes (as for the coherent combining acquisition scheme).

IV. PERFORMANCE STUDY

The performance study is common to the DBZP and DBZPTI acquisition methods. The approach followed herein is the usual Neyman-Pearson's approach that is based on a hypothesis test ([Chibout, 2008]).

Detection threshold

Let's assume that the useful signal is absent and there is only noise.

Hypothesis H0: the useful signal is not present
The acquisition detector in this case is:

$$T_0 = \sum_{k=1}^{K} \left(n_I^2(k) + n_Q^2(k)\right)$$

$$= \sum_{k=1}^{K} \left(\left(\mathcal{R}(n_\iota) - Im(n_\rho)\right)^2 + \left(\mathcal{R}(n_\rho) + Im(n_\iota)\right)^2\right)$$

At the partial correlator output, the noise, b_l, is assumed as white and Gaussian and its variance is noted:

$$\sigma_{I_p}^2 = 2 \times \frac{N_0}{4\frac{t_i}{M}} \text{ (in Eq. 11):}$$

$$b_l \sim \mathcal{N}(0, \sigma_{I_p}^2)$$

So, let's note

$$n_\iota(k) = \sum_{l=0}^{M-1} b_l e^{-\frac{i2\pi kl}{M}} \in \mathbb{C}$$

So,

$$n_I(k),\ n_Q(k) \quad \sim \quad \mathcal{N}(0, 2\sigma_\iota^2)$$

$$\frac{T_0}{2\sigma_\iota^2} = \sum_{k=1}^{K} \frac{\left(n_I^2(k) + n_Q^2(k)\right)}{2\sigma_\iota^2} \quad \sim \quad \chi^2(2K)$$

Equation 18

where

- $\sigma_\iota^2 = var\left(\mathcal{R}\left(n_\iota(k)\right)\right) = \frac{1}{2}M\sigma_{I_p}^2 = \frac{1}{2}M \times 2\frac{N_0}{4\frac{t_i}{M}}$

Then, $\frac{T_0}{2\sigma_\iota^2}$ is a χ^2 distribution with $2K$ degrees of freedom.

The false alarm probability is the probability that the signal is present (the threshold is crossed) whereas it is not present (only noise is present):

$$P_{fa} = P_{H_0}(H_1) = P_{H_0}(T_o > T_h)$$
$$= P_{H_0}\left(Z > \frac{T_h}{2\sigma_\iota^2}\right) \text{ where } Z \sim \chi^2(2K)$$

Equation 19

So the threshold T_h can easily be deduced by inverting $f_Z(P_{fa})$ for a predefined value of P_{fa}.

Probability of detection

Let's now assume that the useful signal is present.

Hypothesis H1: the useful signal is present

In case of the useful signal is present and that only noise is present, the test statistic has the following expression:

$$T_1 = \sum_{k=1}^{K} \left(I^2(k) + Q^2(k)\right)$$

So,

$$I(k), Q(k) \sim \mathcal{N}\left(\lambda_{k,I/Q}, 2\sigma_\iota^2\right)$$

$$\frac{T_1}{2\sigma_\iota^2} = \sum_{k=1}^{K} \left(\left(\frac{I(k)}{\sqrt{2\sigma_\iota^2}}\right)^2 + \left(\frac{Q(k)}{\sqrt{2\sigma_\iota^2}}\right)^2\right) \sim \chi^2(2K, \lambda)$$

Equation 20

where

- $\lambda_{k,I} = E\left[\frac{I(k)}{\sqrt{2\sigma_\iota^2}}\right] = E\left[\frac{\mathcal{R}(\iota(k)) - Im(\rho(k))}{\sqrt{2\sigma_\iota^2}}\right]$ is the bias of normalized I
- $\lambda_{k,Q}$ is the bias of normalized Q
- $\lambda = \sum_{k=1}^{K}\left(\lambda_{k,I}^2 + \lambda_{k,IQ}^2\right)$ is the non-centrality parameter

Then, λ can be can be rewritten as:

$$\lambda = \frac{A^2}{2\sigma_\iota^2} KM^2R^2\left(\varepsilon_\tau(k)\right) sinc^2\left(\frac{\pi t_i}{M} f_D\right) \left(\frac{\text{sinc}(\pi(m - f_D t_i))}{\text{sinc}\left(\frac{\pi(m - f_D t_i)}{M}\right)}\right)^2$$
$$\approx 2\frac{A^2}{N_0} t_i K R^2\left(\varepsilon_\tau(k)\right) sinc^2\left(\frac{\pi t_i}{M} f_D\right) \left(\frac{\text{sinc}(\pi(m - f_D t_i))}{\text{sinc}\left(\frac{\pi(m - f_D t_i)}{M}\right)}\right)^2$$

Equation 21

So, the test statistic $\frac{T_1}{2\sigma_\iota^2}$ is a non central χ^2 distribution with $2K$ degrees of freedom and a non-centrality parameter λ. The probability of detection is:

$$P_d = P_{H_1}(H_0) = P_{H_1}(T_1 > T_h)$$
$$= P_{H_1}\left(Z > \frac{T_h}{2\sigma_\iota^2}\right) \text{ where } Z \sim \chi^2(2K, \lambda)$$

Equation 22

The probability of detection depends on the total C/N_0 at the antenna output through λ.

To analyze the performance of the method and compare it with the Reference Acquisition (RA) previously defined, it is interesting to study the probability of detection of the two methods for a given probability of false alarm and received C/N_0. The constraints set here is that the Galileo E1 OS signals with a C/N_0 of 27 dBHz should be acquired 90% of the time. The probability of false alarm is fixed to $1e^{-3}$.

As seen earlier, the probability of detection of the DBZP and DBZPTI depends on the incoming Doppler frequency through the non-centrality parameter (λ, Eq. 21). As a result, to determine the global probability of detection for the DBZPTI acquisition method, the average value of the probability of detection is evaluated for all possible Doppler frequencies. As a first approximation, the distribution of the possible Doppler frequency values is assumed uniform. For a set of non-coherent summations between 1 and 50, the global probability of detection was thus computed and is reported in the Figure 18. It can be seen that the number of non-coherent summations for the same probability of detection (for example 0.9) is higher in the case of the DBZPTI than for the Reference Acquisition method. This highlights the strong DBZP drawback linked to its susceptibility of the incoming Doppler frequency.

Number of non-coherent summations

To reach of goals, the number of non-coherent summations for the DBZPTI should be $K = 40$ while the number of non-coherent summations for the Reference Acquisition should be $K = 13$. The number of non-coherent summations required for the DBZPTI is thus

significantly higher than that required for the Reference Acquisition.

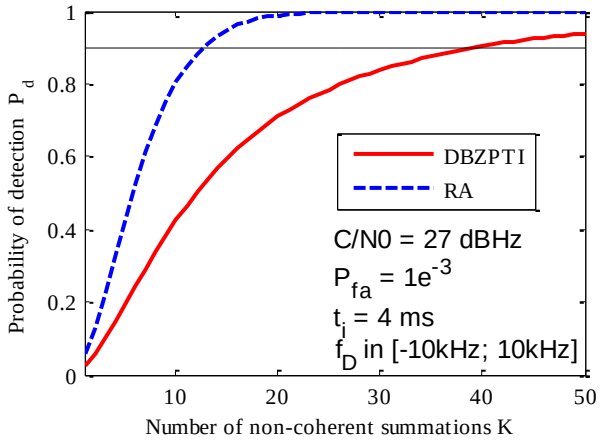

Figure 18 - Probability of detection versus the number of non-coherent integration

However, Figure 18 is valid only is there is no bit transition and does not take into account the bit sensitivity of the Reference Acquisition technique. On the other hand, the DBZPTI being bit insensitive, its performance is represented, as well as the fact that it will not suffer from potential false acquisition on wrong bins due to frequent bit transition.

Simulation results

A Galileo E1 OS signals with a C/N_0 of 27 dBHz were simulated. The simulated incoming Doppler frequency equals $f_D = 1000\,Hz$ (favorable case for the two kinds of acquisition methods) and the code delay is randomly chosen between 0 and 4 ms. 20 occurrences with bit transitions were generated. The DBZPTI acquisition algorithm was run each time with 40 non-coherent summations and the Reference Acquisition with 13 non-coherent summations. The results show that the right code delay (plus or minus ¼ chip) and the right Doppler frequency (with an uncertainty of 375 Hz) is five times more detected with the DBZPTI (with 40 non-coherent summations) than with the Reference Acquisition (with 13 non-coherent summations).

Furthermore, the total acquisition computation time of the DBZPTI (although the number of non-coherent summations is higher than this of the Reference Acquisition) is lower (divided by approximately 1.5) than that of the Reference Acquisition.

CONCLUSION

This paper derived the mathematical expression of outputs of the different steps of the Double Block Zero Padding which is has not been published in the literature to the author's knowledge. These mathematical models allowed understanding the rationale being the DBZP and investigating the performance of the method compared to a reference acquisition technique. It highlighted several interesting points:

- The DBZP is bit transition sensitive
- The SNR at the DBZP output is comparable to the SNR at the output of a traditional correlator used by the Reference Acquisition.
- The performance of the DBZP sharply depends on the incoming Doppler frequency (losses for high frequencies in absolute value and for frequencies exactly between two frequency bins)
- The DBZP is computationally efficient. A detailed computation of the number of elementary operations for the DBZP is presented

The second part of this work was the development of a new Galileo E1 OS acquisition method. This method is based on the DBZP and was referred to as the Double Block Zero Padding Transition Insensitive (DBZPTI) as it is not sensitive to the frequent bit transition present in the Galileo E1 OS signal on both the data and pilot components. The computational efficiency of the DBZPTI is equivalent to that of the DBZP and allows saving a considerable amount of time for the total acquisition process. Nonetheless, the DBZPTI presents the drawback (intrinsic to the DBZP) that its performance (in terms of sensitivity) depends strongly upon the incoming Doppler frequency.

ACKNOWLEDGMENTS

The authors would like to thank the G-TRAIN project (funded by the EC/EUROPEAN GNSS AGENCY (GSA) under the FP7, through the Satellite navigation University Network (SUN) activities for PhDs (Msc) students) which partially supported the presenter's attendance to the conference.

REFERENCES

AL BITAR, H., (2007), *Advanced GPS signal processing techniques for LBS services*, PhD Thesis, ENAC, Toulouse, France.

BASTIDE, F., E. TESA, C. MACABIAU, AND B. ROTURIER, (2002), *ANALYSIS OF L5 / E5 ACQUISITION , TRACKING AND DATA DEMODULATION*, Signalsp.24–27.

BORIO, D., AND L. LO PRESTI, (2008), *Data and Pilot Combining for Composite GNSS Signal Acquisition*, International Journal of Navigation and Observation 2008: p.1–12.

BORRE, K., D.M. AKOS, N. BERTELSEN, P.J. RINDER, AND S.H. JENSEN, (2007), *A software-defined GPS and Galileo receiver, A single-frequency approach* Birhäuser.,

CHIBOUT, B., (2008), *Application of indoor and urban GNSS localisation techniques to space navigation*, PhD Thesis, ENAC, Toulouse, France.

CORAZZA, G.E., C. PALESTINI, R. PEDONE, AND M. VILLANTI, (2006), *Galileo primary code acquisition based on multi-hypothesis secondary code ambiguity elimination*, International Journal of Satellite Communications and Networking 24: p.153–167.

FANTINO, M., G. MARUCCO, P. MULASSANO, AND M. PINI, (2008), *Performance Analysis of MBOC , AltBOC and BOC Modulations in Terms of Multipath Effects on the Carrier Tracking Loop within GNSS Receivers*, Powerp.369–376.

GPS WORLD, (2012), *Receiver Survey 2012, sponsored by Novatel*, GPS World January 2012.

JULIEN, O., (2008), *ENGO 638: GNSS RECEIVER DESIGN* in Lecture Notes ENGO, August 18, Department of Geomatics Engineering, University of Calgary.

LIN, D., AND J.B.Y. TSUI, (2000), *Comparison of acquisition methods for software GPS receiver* in ION GPS 2000, September 19, Salt Lake City, UT.

LIN, D.M., AND J.B.Y. TSUI, (1998), *Acquisition schemes for sofware GPS receiver* in ION GPS 1998, September 15, Nasville, TN.

LIN, D.M., J.B.Y. TSUI, AND T. HOWELL, (1999), *Direct P(Y)-code acquisition algorithm for software GPS receivers* in ION GPS 99, September 14, Nashville, TN.

LIN, Y., AND S. JAN, (2007), *Multi-C / A Code Acquisition Method* in National Technical Meeting of the Institute of Navigation, January 22, San Diego, CA.

VAN NEE, D., AND A. COENEN, (1991), *New fast GPS code-acquisition technique using FFT*, Electronics Letters 27: p.158–160.

SPILKER, J.J., B. PARKINSON, P. AXELRAD, P. ENGE, AND A.J. VAN DIERENDONCK, (1996), *Global Positioning System: Theory and Applications* Progress in Astronautics and Aeronautics.,

SUN, K., AND L. LO PRESTI, (2010), *A differential post detection technique for two steps GNSS signal acquisition algorithm* in May 4, Indian Wells, CA.

TAWK, Y., A. JOVANOVIC, J. LECLÈRE, C. BOTTERON, AND P.-A. FARINE, (2011), *A New FFT-based algorithm for secondary code acquisition for Galileo signals* in Vehicular Technology Conference (VTC Fall), September 5.

TSUI, J.B.-Y., (2004), *Fundamentals of Global Positioning System Receivers: A Software Approach* Wiley Series in Microwave and Optical Engineering.,

WALLNER, S., J.-A. AVILA-RODRIGUEZ, G.W. HEIN, AND J.J. RUSHANAN, (2007), *Galileo E1 OS and GPS L1C pseudo random noise codes-requirements, generation, optimization and comparison* in Proceedings of the 20th International Technical Meeting of the Satellite Division of The Institute of Navigation (ION GNSS 2007), September 25, Fort Worth, TX.

APPENDICES

Appendix A: Strategy of Galileo E1 OS acquisition

The Table 2 evaluates all data and secondary code bits combination and gives the code equivalent sequence through the value of α.

Table 2 - Data and secondary code bits combinations

	$c_2(k)=1$	$c_2(k)=-1$
$d(k)=1$	$\boldsymbol{\alpha=-1}$ $d(k)+c_2(k)=2$ $R_{c_{1,D}}+R_{c_{1,P}}-2R_{c_{1,D/P}}$	$\boldsymbol{\alpha=1}$ $d(k)+c_2(k)=0$ $R_{c_{1,D}}+R_{c_{1,P}}+2R_{c_{1,D/P}}$
$d(k)=-1$	$\boldsymbol{\alpha=1}$ $d(k)+c_2(k)=0$ $-\left(R_{c_{1,D}}+R_{c_{1,P}}\right)-2R_{c_{1,D/P}}$	$\boldsymbol{\alpha=-1}$ $d(k)+c_2(k)=-2$ $-\left(R_{c_{1,D}}+R_{c_{1,P}}\right)+2R_{c_{1,D/P}}$

Appendix B: Sum of an exponential geometric series

An important and useful result is:

$$\sum_{n=1}^{N} e^{i2\pi\alpha n} = Ne^{i\pi\alpha(N-1)}\frac{sinc(\pi\alpha N)}{sinc(\pi\alpha)}$$

The proof is:

$$\sum_{n=1}^{N} e^{i2\pi\alpha n} = \frac{1-e^{i2\pi\alpha N}}{1-e^{i2\pi\alpha}} = \frac{e^{i\pi\alpha N}(e^{-i\pi\alpha N}-e^{i\pi\alpha N})}{e^{i\pi\alpha}(e^{-i\pi\alpha}-e^{i\pi\alpha})}$$

$$= e^{i\pi\alpha(N-1)}\frac{sin(\pi\alpha N)}{sin(\pi\alpha)} = Ne^{i\pi\alpha(N-1)}\frac{sinc(\pi\alpha N)}{sinc(\pi\alpha)}$$

Appendix C: Circular correlation

Correlation function

The general expression of the correlation is:

$$R(m) = \frac{1}{N}\sum_{l=0}^{N-1} c(l)c(l-m)$$

But $c(l)$ can be expressed as a decomposition in Fourier series:

$$c(l) = \frac{1}{N}\sum_{n=0}^{N-1} C(n)e^{i2\pi ln/N}$$

And so:

$$R(m)$$

$$= \frac{1}{N}\sum_{l=0}^{N-1}\left(\frac{1}{N}\sum_{n=0}^{N-1} C(n)e^{i2\pi ln/N}\right)\left(\frac{1}{N}\sum_{p=0}^{N-1} C(p)e^{i2\pi(l-m)p/N}\right)$$

$$= \frac{1}{N}\frac{1}{N^2}\sum_{n=0}^{N-1}\sum_{p=0}^{N-1} C(n)C(p)e^{-\frac{i2\pi mp}{N}}\sum_{l=0}^{N-1} e^{i2\pi l(n+p)/N}$$

If $n+p \neq 0$ then $\sum_{l=0}^{N-1} e^{i2\pi l(n+p)/N} = 0$

If $n+p=0$, then $p=-n$ then $\sum_{l=0}^{N-1} e^{i2\pi l(n+p)/N} = N$ and :

$$R(m) = \frac{1}{N}\frac{1}{N^2}N\sum_{n=0}^{N-1} C(n)C(-n)\,e^{-i2\pi m(-n)/N}$$

$$= \frac{1}{N}IFFT\big(C(n)C(-n)\big)$$

$$= \frac{1}{N}IFFT\big(FFT\big(c(k)\big)\overline{FFT}(c(k))\big)$$

Because

$$C(-n) = \frac{1}{N}\sum_{k=0}^{N-1} c(k)e^{-i2\pi(-n)k/N} = \frac{1}{N}\sum_{k=0}^{N-1} c(k)e^{-i2\pi(-n)k/N}$$

$$= \frac{1}{N}\sum_{k=0}^{N-1} c(k)e^{i2\pi nk/N} = \overline{\frac{1}{N}\sum_{k=0}^{N-1} c(k)e^{-\imath 2\pi nk/N}} = \overline{FFT}\big(c(k)\big)$$

Appendix D: Circular correlation

Let's note

$$k=0\ldots N-1$$

The FFT of the signal is:

$$FFT\big(r(t)\big)(k) = \sum_{n=0}^{N-1} r(n)e^{-i2\pi kn/N}$$

And the complex conjugate of the FFT of the code is:

$$FFT\big(c(t)\big)(k) = \sum_{n=0}^{N-1} c(n)e^{i2\pi kn/N}$$

The product of the two FFT is:

$$\left(FFT\big(r(t)\big)\,\overline{FFT}\big(c(t)\big)\right)(k)$$

$$= \sum_{n=0}^{N-1} r(n)e^{-i2\pi kn/N}\sum_{m=0}^{N-1} c(m)e^{-i2\pi km/N}$$

$$= \sum_{n=0}^{N-1}\sum_{m=0}^{N-1} r(n)c(m)e^{i2\pi k(m-n)/N}$$

Taking the inverse Fast Fourier Transform:

$$IFFT\left(FFT\big(r(t)\big)\,\overline{FFT}\big(c(t)\big)\right)(j)$$

$$= \frac{1}{N}\sum_{k=0}^{N-1}\left(\sum_{n=0}^{N-1}\sum_{m=0}^{N-1} r(n)c(m)e^{i2\pi k(m-n)/N}\right)e^{i2\pi kj/N}$$

$$= \frac{1}{N}\sum_{n=0}^{N-1}\sum_{m=0}^{N-1} r(n)c(m)\sum_{k=0}^{N-1} e^{i2\pi k(m-n+j)/N}$$

$$= \frac{1}{N}\sum_{n=0}^{N-1} r(n)c(n-j)$$

because $\sum_{k=0}^{N-1} e^{i2\pi k(m-n+j)/N}$ is equal to 0 if $m-n+j = 0 \iff m = n-j$

And with the introduction of the autocorrelation function by means of an expectation

$$
\begin{aligned}
&\sum_{n=0}^{N-1} r(n)c(n-j) \\
= &\frac{A}{2}\sum_{n=0}^{N-1} d(t_n-\tau)\cos\left(2\pi\varepsilon_{f_D}t_n+\varepsilon_{\phi_0}\right)c(t_n-\tau)c(t_n-jT_s) \\
&+\frac{A}{2}\sum_{n=0}^{N-1} n(t_n)c(t_n) \\
= &\frac{A}{2}N\sum_{n=0}^{N-1} d(t_n-\tau)\cos\left(2\pi\varepsilon_{f_D}t_n+\varepsilon_{\phi_0}\right)R(\tau-jT_s) \\
&+\frac{A}{2}\sum_{n=0}^{N-1} n(t_n)c(t_n-jT_s) \\
= &\frac{A}{2}Nd(t_0-\tau)R(\tau-jT_s)\sum_{n=0}^{N-1}\cos\left(2\pi\varepsilon_{f_D}t_n+\varepsilon_{\phi_0}\right) \\
&+\frac{A}{2}\sum_{n=0}^{N-1} n(t_n)c(t_n-jT_s) \\
= &\frac{AN}{2}d(t_0-\tau)R(\tau-jT_s)\left(2\cos\left(\varepsilon_{\phi_0}+\pi\varepsilon_{f_D}T_s(N-1)\right)\frac{\sin\left(N\pi\varepsilon_{f_D}T_s\right)}{\sin\left(\pi\varepsilon_{f_D}T_s\right)}\right) \\
&+\frac{A}{2}\sum_{n=0}^{N-1} n(t_n)c(t_n-jT_s)
\end{aligned}
$$

By assuming that $\mathrm{d}(\mathrm{t_n}-\tau)$ and $\varepsilon_{\phi_\mathrm{n}}$ are constants over an integration period.

Appendix E: DBZP outputs

Let's note ϕ and $\hat{\phi}$ the phase of the incoming signal and of the local carrier:

$$\phi = 2\pi(f_0+f_D)t+\phi_0$$
$$\hat{\phi} = 2\pi t f_0+\widehat{\phi_0}$$

where

- f_0 is the frequency of the signal in baseband
- ϕ_0 is the phase at the instant 0

So the difference between the incoming phase and the local phase is:

$$
\begin{aligned}
&\phi-\hat{\phi} \\
= &\ 2\pi f_D t+\phi_0-\widehat{\phi_0} \\
= &\ 2\pi f_D t+\varepsilon_{\phi_0}
\end{aligned}
$$

where

- ε_{ϕ_0} is the difference of the initial phases

Let's note M_s the number of samples. The components of the correlated signal are assumed as random and so the correlator output can be seen as the mean of the accumulated samples.

$$
\begin{aligned}
&I \\
= &\ E\left[\sum_{k=1}^{M_S}\frac{A(k)}{2}c(k-\tau)\,c(k)\cos\left(\phi(k)-\hat{\phi}(k)\right)\right] \\
= &\ \frac{A}{2}R_p\left(\varepsilon_\tau(k)\right)\sum_{k=1}^{M_S}\cos\left(\phi(k)-\hat{\phi}(k)\right)
\end{aligned}
$$

Moreover, the sum of cosine can be approximated by a numeric integral on the interval $\left[t_0+l\frac{t_i}{M};t_0+(l+1)\frac{t_i}{M}\right]$:

$$
\begin{aligned}
&I \\
= &\ \frac{1}{\frac{t_i}{M}}\frac{A}{2}R_p\left(\varepsilon_\tau(k)\right)\int_{t_0+l\frac{t_i}{M}}^{t_0+(l+1)\frac{t_i}{M}}\cos\left(\left(\phi(t)-\hat{\phi}(t)\right)\right)dt \\
= &\ \frac{1}{\frac{t_i}{M}}\frac{A}{2}R_p\left(\varepsilon_\tau(k)\right)\int_{t_0+l\frac{t_i}{M}}^{t_0+(l+1)\frac{t_i}{M}}\cos\left(2\pi f_D t+\varepsilon_{\phi_0}\right)dt \\
= &\ \frac{A}{2}R_p\left(\varepsilon_\tau(k)\right)\frac{1}{2}\frac{1}{\pi f_D\frac{t_i}{M}}\left[\sin\left(2\pi f_D t+\varepsilon_{\phi_0}\right)\right]_{t_0+l\frac{t_i}{M}}^{t_0+(l+1)\frac{t_i}{M}} \\
= &\ \frac{A}{2}R_p\left(\varepsilon_\tau(k)\right)sinc\left(\pi f_D\frac{t_i}{M}\right)\cos\left(2\pi f_D\left(t_0+\frac{t_i}{M}\left(l+\frac{1}{2}\right)\right)+\varepsilon_{\phi_0}\right)
\end{aligned}
$$

Finally, the expression of the l[th] partial correlator outputs is:

$$
\begin{cases}
\widetilde{I_p}(l,k) = n_{\widetilde{I_p}}(l,k)+ \\
\dfrac{A}{2}R_p\left(\varepsilon_\tau(k)\right)sinc\left(\pi f_D\dfrac{t_i}{M}\right)\cos\left(2\pi f_D\left(t_0+\dfrac{t_i}{M}\left(l+\dfrac{1}{2}\right)\right)+\varepsilon_{\phi_0}\right) \\
\widetilde{Q_p}(l,k) = n_{\widetilde{Q_p}}(l,k)+ \\
\dfrac{A}{2}R_p\left(\varepsilon_\tau(k)\right)sinc\left(\pi f_D\dfrac{t_i}{M}\right)\sin\left(2\pi f_D\left(t_0+\dfrac{t_i}{M}\left(l+\dfrac{1}{2}\right)+\varepsilon_{\phi_0}\right)\right)
\end{cases}
$$

Appendix F: *DBZP output with a transition*

The computation of the FFT of the cosine when a data transition occurs is given hereafter. The partial correlator output depends on the data bit represented by $d(l)$. For the development, we fix that $d(l)=1$ for $l=1\ldots L$ and $d(l)=-1$ for $l=L+1\ldots M$. That means that a transition occurs at L.

$$
\begin{aligned}
&FFT\left(d(l)cos\left(2\pi f_D\left(t_0+\frac{lt_i}{M}+\frac{t_i}{2M}\right)+\varepsilon_{\phi_0}\right)\right)\left(m_{m=0\ldots M-1}\right) \\
= &\sum_{l=0}^{M-1} d(l)cos\left(2\pi f_D\left(t_0+\frac{lt_i}{M}+\frac{t_i}{2M}\right)+\varepsilon_{\phi_0}\right)e^{-\frac{i2\pi ml}{M}} \\
= &\sum_{l=0}^{L-1} cos\left(2\pi f_D\left(t_0+\frac{lt_i}{M}+\frac{t_i}{2M}\right)+\varepsilon_{\phi_0}\right)e^{-\frac{i2\pi ml}{M}} \\
&-\sum_{l=L}^{M-1} cos\left(2\pi f_D\left(t_0+\frac{lt_i}{M}+\frac{t_i}{2M}\right)+\varepsilon_{\phi_0}\right)e^{-\frac{i2\pi ml}{M}} \\
= &\ \frac{1}{2}e^{i\left(2\pi f_D\left(t_0+\frac{t_i}{2M}\right)+\varepsilon_{\phi_0}\right)}\left(-\sum_{l=0}^{L-1}e^{-\frac{i2\pi}{M}l(m-f_D t_i)}+\sum_{l=L}^{M-1}e^{-\frac{i2\pi}{M}l(m-f_D\,t_i)}\right) \\
&+\frac{1}{2}e^{-i\left(2\pi f_D\left(t_0+\frac{t_i}{2M}\right)+\varepsilon_{\phi_0}\right)}\left(-\sum_{l=0}^{L-1}e^{-\frac{i2\pi}{M}l(m+f_D t_i)}+\sum_{l=L}^{M-1}e^{-\frac{i2\pi}{M}l(m+f_D t_i)}\right) \\
= &\ \frac{1}{2}e^{i\left(2\pi f_D\left(t_0+\frac{t_i}{2M}\right)+\varepsilon_{\phi_0}\right)}\frac{\mathrm{sinc}(\pi(m-f_D t_i))}{\mathrm{sinc}\left(\frac{\pi(m-f_D t_i)}{M}\right)} \\
&\times\left(-Le^{-i\pi\frac{(L-1)}{M}(m-f_D t_i)}+(M-L)e^{-i\pi\frac{(M-L-1)}{M}(m-f_D t_i)}\right) \\
&+\frac{1}{2}e^{-i\left(2\pi f_D\left(t_0+\frac{t_i}{2M}\right)+\varepsilon_{\phi_0}\right)}\frac{\mathrm{sinc}(\pi(m+f_D t_i))}{\mathrm{sinc}\left(\frac{\pi(m+f_D t_i)}{M}\right)} \\
&\times\left(-Le^{-i\pi\frac{(L-1)}{M}(m+f_D t_i)}+(M-L)e^{-i\pi\frac{(M-L-1)}{M}(m+f_D t_i)}\right)
\end{aligned}
$$

Appendix G: Number of operations

The Table 3 gives the number of elementary operations for the two acquisitions methods: DBZP and reference acquisition (RA). For the computation of a FFT on a vector of size N, there are $\frac{N}{2}\log_{10}(N)$ multiplications and

$N \log_{10}(N)$ additions. The number of operations for one acquisition is divided by 2.2 for the DBZP with regard to the Reference Acquisition.

Table 3 - Number of operations for the two acquisition methods

			Size of vector	Operations		Multiplications	Additions	Elementary operations	TOTAL
DBZP	signal.*exp(.)	Step 1	81920	3		2,5E+05	8,2E+04	3,3E+05	
	FFT(signal)		2048	159		5,4E+05	1,1E+06	1,6E+06	
	FFT(code)	Step 3	2048	80		2,7E+05	5,4E+05	8,1E+05	
	FFT*FFT		2048	6400		1,3E+07		1,3E+07	**1,3E+08**
	IFFT		2048	6400		2,2E+07	4,3E+07	6,5E+07	
	Last FFT	Step 4	80	81920		6,2E+06	1,2E+07	1,9E+07	
	Squaring		7E+06	2		1,3E+07	1,3E+07	2,6E+07	
RA	signal.*exp(.)		81920	483		4,0E+07	8,3E+04	4,0E+07	
	FFT(signal)		81920	161		3,2E+07	6,5E+07	9,7E+07	
	FFT(code)		81920	1		2,0E+05	4,0E+05	6,0E+05	
	FFT*FFT		81920	161		1,3E+07		1,3E+07	**2,7E+08**
	IFFT		81920	161		3,2E+07	6,5E+07	9,7E+07	
	Squaring		81920	161		1,3E+07	1,3E+07	2,6E+07	